

# Effect of the geometry of the porous material pore surface on mechanical properties

© G.A. Nikiforov, B.N. Galimzyanov, A.V. Mokshin

Kazan Federal University,  
420008 Kazan, Russia  
e-mail: nikiforov121998@mail.ru

Received May 3, 2024

Revised August 4, 2024

Accepted October 30, 2024

The effect of the geometry of the pore surface in a porous material on its mechanical properties, such as Young's modulus and tensile strength, has been studied. The study was carried out using the molecular dynamics modeling method using the example of porous titanium nickelide at porosity values of 52, 62.5 and 73%. It is shown that a material with a concave pore surface has better resistance to external loads. The analysis of differences in the morphology of materials with different surface geometries using distributions of linear pore sizes and interstitial partitions was also carried out.

**Keywords:** mechanical properties, porous materials, titanium nickelide, molecular dynamics.

DOI: 10.61011/TP.2024.12.60392.395-24

## Introduction

Porous materials are actively studied and used in many industries and medicine [1–3]. For example, the porous materials with the open type of pores are used for heat insulation and as a catalyst due to the higher specific surface area, as materials for implants because of better integration with the live tissues. In addition to the heat insulation properties, the materials with the closed type of pores are used to make dampers. Mechanical and physical properties of the porous material are determined both by the properties of a hard matrix and the parameters of the porous system. Such parameters include porosity, distributions of linear dimensions of pores and interpore partitions, morphology features. The morphology features may include the spatial distribution of the hard matrix. Thus, papers [4,5] studied the dependence of the mechanical properties on the even distribution of the hard matrix along the direction of the applied load. The Young's modulus and ultimate tensile strength increase was noted. This paper will study the impact of such morphology feature as the geometry of the pore surface at the mechanical properties of the porous titanium nickelide.

## 1. Simulation details

The method of molecular dynamics simulation produced the porous systems, the interpore partitions of which had both convex and concave surfaces (fig. 1). Note that in practice the morphology of the porous material with the concave surface is obtained using gas injection into the melt [6–8]. The morphology with the convex surface is obtained as a result of powder sintering [9]. For every morphology the specimens were simulated with porosity  $52.0 \pm 2.0\%$ ,  $62.5 \pm 2.5\%$ ,  $73.0 \pm 2.0\%$  with the open type of pores. The porous systems were produced with

the help of atoms removal from the crystalline base. To obtain the porous structure with the concave surface of the pores, ellipsoids were cut from the material with the specified linear dimensions in a random manner. At porosity above 50% the randomly cut pores form a network of the crossing capillaries. The obtained morphology of the porous structure qualitatively follows the morphology of the porous experimental specimens [4,5]. When the porous structure was produced with the convex surface of the pores, a network of the crossing threads with the specified thickness was separated from the monolithic system. Such threads were made by continuous serial imposition of the ellipsoids along the random trajectory. The atoms beyond the network of the threads were removed. This made it possible to approach the qualitative similarity of the morphology of the porous system produced by powder sintering. All specimens were brought into the equilibrium state for 100 ps in the martensite phase. The interatomic interaction was given by the potential 2NN MEAM [10]. This potential reproduces the structure and physical properties of titanium nickelide with good precision in the wide area of pressures and temperatures [11,12]. The stretching took place along axis  $Ox$  at a temperature of 300 K with a strain rate  $\dot{\epsilon} = 5 \cdot 10^9 \text{ s}^{-1}$  in the NVT ensemble. Such scale of strain rates is acceptable for the method of molecular dynamics modeling.

## 2. Discussion of results

For the produced porous systems the distributions of linear dimensions of pores  $d$  and interpore partitions  $l$  (fig. 2) were obtained, as well as their average values  $\bar{d}$  and  $\bar{l}$  accordingly (table 1). The average values of linear dimensions of pores  $\bar{d}$  and interpore partitions  $\bar{l}$  directly impact the mechanical characteristics [13,14]. Based on the data given in table 1, one can see the difference in

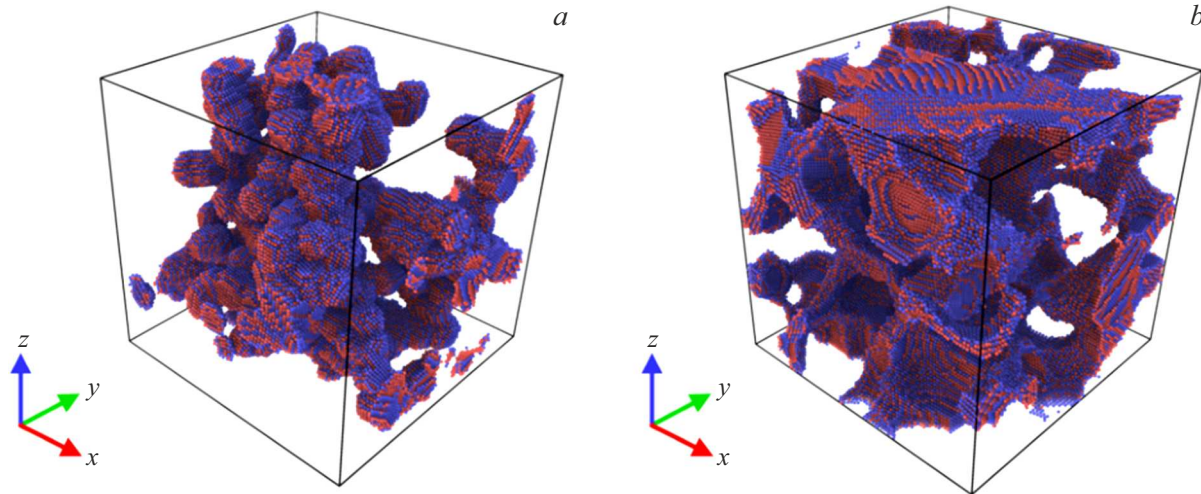


**Figure 1.** Snapshots of the porous system with porosity  $72.0 \pm 2.0\%$  with convex (a) and with concave (b) surfaces.

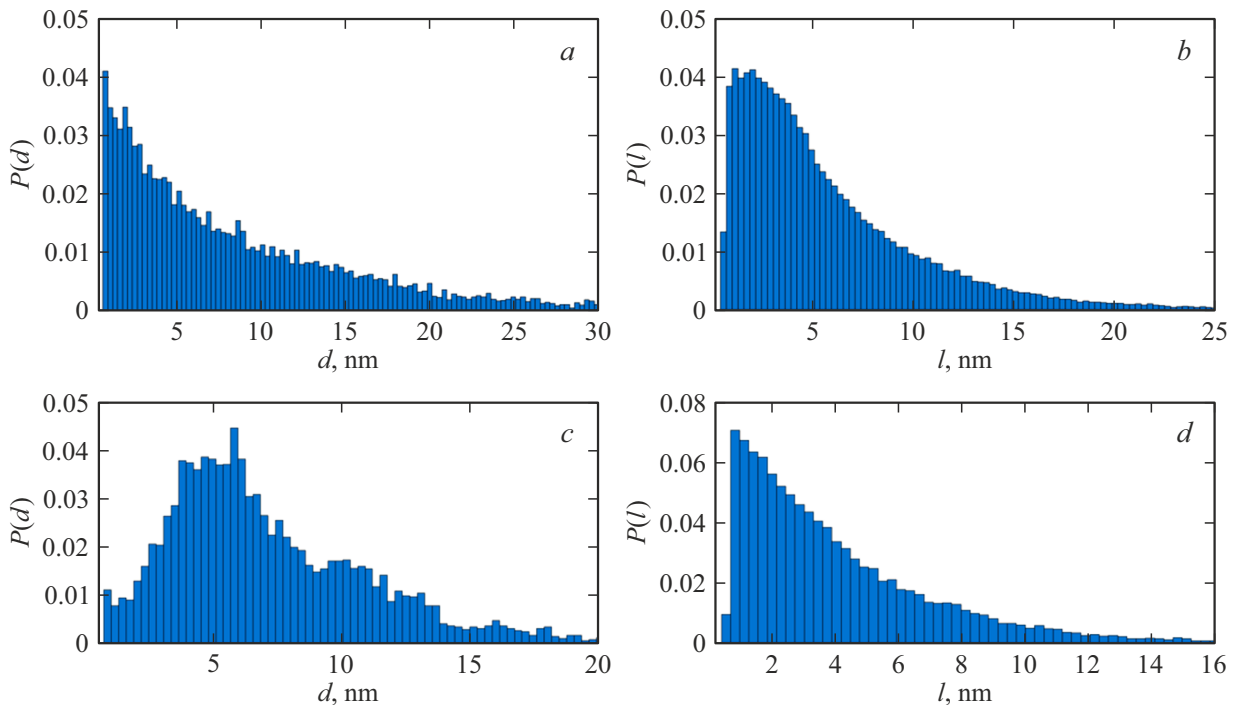


**Figure 2.** Distributions of linear dimensions of pores  $P(d)$  and partitions  $P(l)$  for systems ( $\phi = 62.5 \pm 2.5\%$ ) with convex (a, b) and concave (c, d) surfaces.

the average linear dimensions of the pores and inter-pore partitions for the systems with the same porosity, but different curvature of the pore surfaces. Thus, at porosity of  $52.0 \pm 2.0\%$  the average linear size of the pores for the convex surface of the pores is 20% less than for the concave one. In its turn the average linear dimensions of the inter-pore partitions are the same. But at porosity of  $62.5 \pm 2.5\%$  the average linear size of the pores for the convex surface of pores is 21% larger, and the average linear size of the inter-pore partitions is larger by 41%. At porosity of  $73.0 \pm 2.0\%$  the trend changes again. The average linear size of the pores and inter-pore partitions for the convex

surface is smaller by 6.5 and 9.5% accordingly. Based on the produced data during this study, the correlation between the morphology of the porous material surface and average linear dimensions of the pores and inter-pore partitions was not found. The latter to a large extent are determined by the porosity value of  $\phi$ . But the shape of distributions of the linear dimensions of the pores and inter-pore partitions differs. For the systems with the concave surface, there is a marked dome-shaped maximum for the distribution of the linear dimensions of pores. Besides, the distribution of the linear dimensions of the inter-pore partitions is characterized by the presence of preferably thin partitions, which is

**Table 1.** Parameters of produced porous systems

Surface geometry	$\phi, \%$	$\bar{d}, \text{nm}$	$\bar{l}, \text{nm}$
Concave	$52.0 \pm 2.0$	3.5	3.6
	$62.5 \pm 2.5$	7.1	4.1
	$73.0 \pm 2.0$	9.4	4.3
Convex	$52.0 \pm 2.0$	2.8	3.6
	$62.5 \pm 2.5$	8.6	5.8
	$73.0 \pm 2.0$	8.8	3.9

**Table 2.** Mechanical characteristics of produced systems

Geometry of surface	Porosity, %	$E, \text{GPa}$	$\sigma_{ult}, \text{GPa}$
Concave	$52.0 \pm 2.0$	$16.2 \pm 0.67$	$1.40 \pm 0.80$
	$62.5 \pm 2.5$	$12.6 \pm 2.63$	$0.80 \pm 0.27$
	$73.0 \pm 2.0$	$3.20 \pm 1.74$	$0.34 \pm 0.19$
Convex	$52.0 \pm 2.0$	$10.5 \pm 1.65$	$0.80 \pm 0.20$
	$62.5 \pm 2.5$	$6.25 \pm 2.70$	$0.69 \pm 0.20$
	$73.0 \pm 2.0$	$1.16 \pm 0.18$	$0.24 \pm 0.02$

designated by the monotonic diagram downtrend. For the systems with the convex surface the situation is the reverse, however, the top of the dome on the curve of the partition size distribution is moved to the side of the smaller dimensions.

Table 2 provides the values of the Young's modulus and the ultimate tensile strength. The Young's modulus was calculated as the tangent of the inclination angle of the linear section in the stress–strain curve. The ultimate tensile strength was determined as the maximum stress value in this curve. It was noted that the specified characteristics were higher for the concave surface case. It may be related to the fact that the porous system with the concave surface is more branched, and certain areas of the hard matrix are the stiffening ribs. It was also noted that the ratio of the Young's modulus of the system with the concave surface to the Young's modulus of the system with the convex surface increases as the system porosity increases. It may be explained by the fact that with the porosity growth the hard matrix with the convex surface becomes less even along the identified direction, which reduces the total resistance to the load.

## Conclusion

It was shown that the geometry of the porous material pore surfaces at the fixed porosity may not be clearly determined using only the average values of the linear dimensions of pores and interpore partitions. The structural

differences may be found by analysis of the distributions of the linear dimensions in the specified characteristics. It was also found that the porous materials with the concave surface have higher values of the Young's modulus and ultimate tensile strength compared to the materials with the convex surface. This may be explained by a more branched structure of the hard matrix of the material with the concave surface and presence of the stiffening ribs therein.

## Funding

This study was performed as part of the Program „Priority — 2030“.

## Conflict of interest

The authors declare that they have no conflict of interest.

## References

- [1] A. Thomas. *Nat. Commun.*, **11**, 4985 (2020). DOI: 10.1038/s41467-020-18746-5
- [2] B. Goyal, A. Pandey. *Mater. Today: Proceedings*, **46**, 8196 (2021). DOI: 10.1016/j.matpr.2021.03.163
- [3] S.G. Anikeev, N.V. Artyukhova, M.I. Kaftaranova, V.N. Khodorenko, A.S. Garin, E.S. Marchenko. *Inorganic Mater.*, **59** (2), 123 (2022). DOI: 10.1134/S0020168523020012
- [4] G.A. Nikiforov, B.N. Galimzyanov, A.V. Mokshin. *High Energy Chem.*, **57**, 137 (2023). DOI: 10.1134/S0018143923070287
- [5] G.A. Nikiforov, B.N. Galimzyanov, A.V. Mokshin. *ZhTF*, **93** (12), 1740 (2023) (in Russian). DOI: 10.61011/JTF.2023.12.56808.f217-23
- [6] N. Behymer, K. Morsi. *Metals*, **13** (5), 959 (2023). DOI: 10.3390/met13050959
- [7] B. Parveez, N.A. Jamal, H. Anuar, Y. Ahmad, A. Aabid, M. Baig. *Materials (Basel)*, **15** (15), 5302 (2022). DOI: 10.3390/ma15155302
- [8] A.A. Tsygankov, B.N. Galimzyanov, A.V. Mokshin. *J. Phys. Condens. Matter.*, **34** (41), 414003 (2022). DOI: 10.1088/1361-648X/ac8512
- [9] S.G. Anikeev, N.V. Artyukhova, A.V. Shabalina, S.A. Kulinich, V.N. Hodorenko, M.I. Kaftaranova, V.V. Promakhov, V.E. Gunter. *J. Alloys Compounds*, **900**, 163559 (2022). DOI: 10.1016/j.jallcom.2021.163559
- [10] W.-S. Ko, B. Grabowski, J. Neugebauer. *Phys. Rev. B*, **92** (134107), 1 (2015). DOI: 10.1103/PhysRevB.92.134107
- [11] J. Chen, D. Huo, H.K. Yeddu. *Mater. Res. Express*, **8** (106508), 1 (2021). DOI: 10.1088/2053-1591/ac2b57
- [12] J. Lee, Y.C. Shin. *Metals*, **11**, 1237 (2021). DOI: 10.3390/met11081237
- [13] Y.-T. Jian, Y. Yang, T. Tian, C. Stanford, X.-P. Zhang, K. Zhao. *PLoS ONE*, **10** (6), e0128138 (2015). DOI: 10.1371/journal.pone.0128138
- [15] B.N. Galimzyanov, G.A. Nikiforov, S.G. Anikeev, N.V. Artyukhova, A.V. Mokshin. *Crystals*, **13** (12), 1656 (2023). DOI: 10.3390/cryst13121656

Translated by E.Ilinskaya